Onset of superfluidity in ^{4}He films adsorbed on disordered substrates

P. A. Crowell,* F. W. Van Keuls,† and J. D. Reppy
Laboratory of Atomic and Solid State Physics and Materials Science Center, Clark Hall, Cornell University, Ithaca, New York 14853-2501
(Received 10 December 1996)

We have studied ^{4}He films adsorbed in two porous glasses, aerogel and Vycor, using high-precision torsional oscillator and dc calorimetry techniques. Our investigation focused on the onset of superfluidity at low temperatures as the ^{4}He coverage is increased. Torsional oscillator measurements of the ^{4}He-aerogel system were used to determine the superfluid density of films with transition temperatures as low as 20 mK. Heat capacity measurements of the ^{4}He-Vycor system probed the excitation spectrum of both nonsuperfluid and superfluid films for temperatures down to 10 mK. Both sets of measurements suggest that the critical coverage for the onset of superfluidity corresponds to a mobility edge in the chemical potential, so that the onset transition is the bosonic analog of a superconductor-insulator transition. The superfluid density measurements, however, are not in agreement with the scaling theory of an onset transition from a gapless, Bose glass phase to a superfluid. The heat capacity measurements show that the nonsuperfluid phase is better characterized as an insulator with a gap. [S0163-1829(97)07217-2]

I. INTRODUCTION

For a wide variety of substrates, adsorbed films of ^{4}He thicker than approximately two atomic layers are superfluid at zero temperature. As the temperature is increased, a transition occurs to a nonsuperfluid phase at a critical temperature T_c. Although the details of this transition depend on the topology of the substrate,[1–4] the phase diagrams for films adsorbed on substrates such as Mylar, porous glasses, or packed powders are similar. In each case, there is a line of transition temperatures in the density-temperature plane separating nonsuperfluid from superfluid films. At $T=0$, this line terminates at a *critical coverage* n_c, below which superfluidity does not occur. Only cesium substrates, which are not wetted by ^{4}He,[5] and the atomically ordered substrates graphite and molecular H_2,[6,7] lead to exceptions to this general picture.

Although the existence of a nonzero critical coverage n_c has been known since the earliest experiments on unsaturated ^{4}He films, the onset of superfluidity as a function of coverage at $T=0$ has received much less experimental attention than the superfluid transition at $T=T_c$. This has followed in part from the difficulty in making thermodynamic measurements on extremely thin ^{4}He films, but also from a conviction that the nonsuperfluid film of coverage n_c forms an essentially inert pseudosubstrate for the overlying superfluid film. Most aspects of thin-film superfluidity can indeed be understood without any consideration of the critical coverage n_c, and the ^{4}He coverage is often renormalized by taking the effective density of the film to be $n-n_c$. For example, the superfluid density of films with transition temperatures above 200 mK is observed to be proportional to $n-n_c$ for many substrates.[8]

In contrast to the inert-layer model used for the interpretation of most experiments, there has been considerable theoretical work suggesting that the onset of superfluidity at $T=0$ in ^{4}He films is analagous to a metal-insulator transition in Fermi systems. This approach follows from a suggestion of Hertz, Fleishman, and Anderson[9] and has been pursued in depth by Fisher *et al.*,[10] who exploited the existence of a natural order parameter in Bose systems to develop a scaling theory for the onset of superfluidity in strongly disordered systems. The spirit of this approach is that the onset transition is driven by the competition between exchange, which favors superfluidity, and the *combined* effects of disorder and the repulsive He-He interactions, which favor localization. The localized phase in the case of a ^{4}He film adsorbed on a strongly disordered substrate is presumed to be a ''Bose glass,'' with a gapless excitation spectrum and a correspondingly nonzero compressibility.

This paper presents superfluid density measurements of ^{4}He films adsorbed in aerogel glass and heat capacity measurements of ^{4}He films adsorbed in Vycor for coverages close to the critical coverage n_c and temperatures down to 10 mK. Our measurements demonstrate that the picture of a superfluid-insulator transition developed by Fisher *et al.* and others[11,12] is qualitatively appropriate. The heat capacity measurements, for example, indicate that a nonsuperfluid film is far from inert. In fact, the density of states of the nonsuperfluid film has a characteristic energy which vanishes as the onset transition is approached from *below* in coverage. We do not, however, find good quantitative agreement with the scaling predictions of Fisher *et al.* for the temperature dependence of the heat capacity and the coverage dependence of the superfluid density and the superfluid transition temperature. We find that the nonsuperfluid film is best characterized as an insulator with a gap as opposed to a Bose glass. The scaling behavior of thin superfluid films is complicated by both the large energy scale characteristic of physical adsorption and the existence of the thermodynamic superfluid transition at nonzero temperatures. The thermodynamic transition appears to be the dominant critical point, at least over the temperature and coverage range of our study.

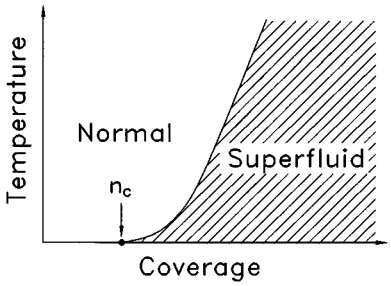

FIG. 1. Generic phase diagram in the density-temperature plane for a ^{4}He film adsorbed on a disordered substrate.

II. BACKGROUND

In Fig. 1 we show a generic phase diagram for an unsaturated ^{4}He film in the temperature-density plane. The film is superfluid at $T=0$ if the coverage exceeds a critical coverage n_c, which is typically 1.5–2 atomic layers. (All of the substrates discussed in this paper are disordered and do not support layer-by-layer growth. An ''atomic layer'' thus corresponds to an average coverage of one layer.) A phase boundary, corresponding to the superfluid transition temperature $T_c(n)$, extends upward from the point $(n=n_c,\ T=0)$. The film is nonsuperfluid above this line. The phase diagram of Fig. 1 is representative of the aerogel and Vycor systems discussed in this paper as well as a variety of other disordered substrates. This paper is devoted to three questions regarding this general phase diagram. First, how can we better understand the onset transition at $n=n_c$: does it have scaling properties like conventional second-order phase transitions? Second, what is the most appropriate description of nonsuperfluid films? Finally, what is our understanding of the thinnest superfluid films, within a few percent of the critical coverage n_c?

A. Bose insulators

One view of the onset transition is that the ^{4}He film is solid at densities below n_c and thus cannot support superfluidity. This viewpoint is equivalent to drawing a vertical line in Fig. 1 at $n=n_c$ and therefore makes a distinction between the ''solid'' part of the film and the ''liquid'' overlayer, which is superfluid at low temperature. Although this approach, often called the ''inert-layer model,'' is sufficient for interpreting most superflow measurements,[8] it eschews particle statistics by ignoring exchange between the solid layer and the overlying superfluid film. In its most orthodox form, the inert-layer model predicts that the various thermodynamic properties of the superfluid should be extensive with respect to $n-n_c$, where n is the total density of the film. In practice, this does not appear to be the case. For example, the superfluid density ρ_s is generally not linear in $n-n_c$ for coverages very close to the onset of superfluidity. This observation has to led to some variations on the inert-layer model, including the suggestion that the compression of the film as it becomes thicker leads to an increase in the density of the inert layer.[13]

A more rigorous approach is difficult, and, although outlined almost 20 years ago,[9] has been pursued in detail only in the last several years. It is quite natural to draw an analogy between the metal-insulator transition in Fermi systems and the onset transition in a ^{4}He film, which is a Bose system. In both cases, one can argue that the onset of metallic (or superfluid) behavior corresponds to the appearance of extended states spanning the system above a critical density n_c. Unfortunately, the theoretical machinery developed for Fermi systems is not readily adaptable to the Bose case because of the strong repulsive interactions. There is no meaningful noninteracting limit, such as pure Anderson localization, for a disordered Bose system.

It is possible, however, to consider a pure but strongly interacting system and then gradually turn on the disorder. The simplest representation of the interactions is a hard-core repulsion V that prevents two atoms from occupying the same site. The effects of quantum exchange are introduced via a hopping matrix element J between different sites. This *Bose-Hubbard model* has been studied for one-dimensional (1D) and two-dimensional (2D) lattice systems.[12] In both cases, the system is ''superfluid'' (meaning a many-body extended state exists) for any density as long as the exchange energy J is greater than a critical value J_c. For weak but nonzero exchange, the system will be superfluid as long as there are sites free to accomodate hopping. This condition fails only at commensurate densities, at which exactly n atoms occupy each site. In this case, the system is localized by the on-site repulsion and is entirely analogous to a Mott insulator in the fermionic case. A gap for particle-hole excitations exists, corresponding to the energy needed to overcome the on-site repulsion when the next atom is added to the system.

Disorder, which can be thought of in the simplest case as a random fluctuation in the on-site repulsion V,[10] has two effects. First, it leads to localization at *incommensurate* densities since atoms will prefer to occupy sites with the lowest on-site repulsion. This can be expected to destroy superfluidity in the case of sufficiently weak exchange. In addition, however, the disorder destroys the Mott insulator at commensurate densities, since the distribution in V implies that the penalty for double occupancy will be reduced at some sites, thus softening the gap. As the strength of disorder is increased further, the gap closes even for small exchange, and the Mott insulator disappears completely. Although the system is now gapless, it is still localized (by disorder) for small exchange strengths. This gapless Bose insulator is often called a *Bose glass*.[9,10]

B. Bose glass to superfluid transition

In the case of porous glasses, the adsorption potential is strongly disordered on the energy scale ($\sim$1 K) characteristic of the exchange in a superfluid ^{4}He film. In this case, the onset of superfluidity within the framework of the Bose-Hubbard model is most likely to occur from the Bose glass phase. A characteristic phase diagram in the plane of exchange strength J and chemical potential μ for the case of strong disorder is shown in Fig. 2. In a real experiment, the chemical potential is tuned by changing the density, and one follows a nearly vertical line in Fig. 2 as the ^{4}He coverage is increased. The onset of superfluidity occurs at the point $\mu=\mu_c$.

The situation sketched in Fig. 2 is reminiscent of a conventional second-order phase transition, with the chemical

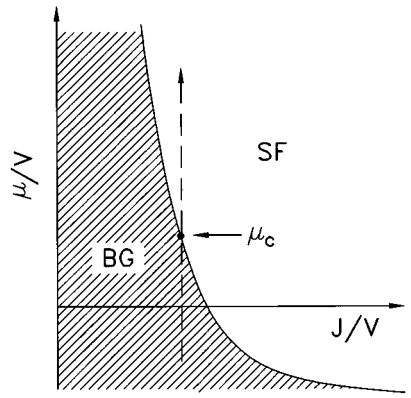

FIG. 2. Phase diagram for the Bose-Hubbard model in the limit of strong disorder in the plane of chemical potential μ and exchange strength J. Both coordinates are scaled by the strength V of the repulsive interaction. The transition from the Bose glass (BG) to the superfluid (SF) phase occurs at the critical chemical potential μ_c as the system travels along a path of nearly constant J, as would be appropriate for the onset transition in a ^{4}He film.

potential μ assuming the role of temperature. Fisher *et al.*[10] have exploited this analogy to construct a scaling theory of the Bose glass to superfluid transition, based on the ansatz that the correlation length ξ for fluctuations in the phase of the order parameter diverges at the onset of superfluidity as

$$\xi \sim \delta^{-\nu}, \tag{1}$$

where the reduced chemical potential $\delta=\mu-\mu_c$ parametrizes the distance to the critical point. Since the number density and the phase of the order paramater are conjugate variables, phase fluctuations are linked to density fluctuations, which propagate at the speed of sound, introducing a time scale as well as the length scale ξ into the problem. Fisher *et al.* define the characteristic frequency Ω, which is assumed to vanish at the onset of superfluidity according to the power law

$$\Omega \sim \xi^{-z}, \tag{2}$$

where z is the *dynamic exponent*. The existence of the dynamic exponent reflects the quantum mechanical origin of the fluctuations in this problem, as opposed to the thermal fluctuations at an ordinary critical point.

Although rigorous arguments are presented by Fisher *et al.*, we note here that conventional hyperscaling will hold if we assume that the correlation volume has a time dimension $(1/\Omega)$ as well as a spatial part ζ^d, where d is the ordinary spatial dimensionality. This allows us to write down an asymptotic form for the singular part f_s of the free energy density at the onset transition:

$$f_s(T=0) \sim \delta^{(d+z)\nu}. \tag{3}$$

An asymptotic form for the *superfluid density* ρ_s on the superfluid side of the transition follows from finite size scaling:[14]

$$\rho_s(T=0) \sim \delta^{\zeta}, \quad \zeta=(d+z-2)\nu. \tag{4}$$

The singular part of the compressibility,

$$\kappa_s=\frac{-\partial^2 f}{\partial \mu^2} \sim \delta^{\nu(d+z)-2}, \tag{5}$$

is analogous to the singular part of the specific heat at a conventional phase transition.

In order to make experimental predictions from these scaling laws, one needs to know the dynamic exponent z. Fisher *et al.* prove that $z=d$ for the case of a Bose glass to superfluid transition. The proof depends critically on the Bose glass having a nonzero compressibility, or, equivalently, a gapless low-energy excitation spectrum.

The theory up to this point makes predictions for the scaling properties of the superfluid density only at $T=0$. Fisher *et al.* have extended their theory to thermodynamic properties at nonzero temperature using finite size scaling in $1/T$. In implementing this argument, they assume that the only energy scale in the problem is set by the characteristic frequency Ω. Temperature will thus appear in the asymptotic free energy in the form $k_BT/\hbar\Omega$. Taking $k_B=\hbar=1$, the scaling form for the free energy becomes

$$f_s(T) \sim \delta^{\nu(d+z)} \tilde{f}(T/\Omega). \tag{6}$$

The superfluid transition (at non-zero temperature) occurs at a universal value u_c of the argument T/Ω, so that

$$T_c = u_c \Omega \sim \delta^{z\nu}. \tag{7}$$

In order to reduce any of the scaling laws into forms testable by experiment, we need to relate $\delta=\mu-\mu_c$ to the density n, which can be tuned in the laboratory. Assuming $z=d$ and using the inequality $\nu \geqslant 2/d$ for the correlation length exponent in disordered systems,[15] it can be shown that

$$n-n_c \sim \mu-\mu_c, \tag{8}$$

which means that δ can be replaced by $n-n_c$ in all of the above scaling laws. After doing so, we obtain the scaling laws of Fisher *et al.*:[10]

$$\rho_s(0) \sim (n-n_c)^{\zeta}, \quad \zeta \equiv \nu(d+z-2), \tag{9}$$

$$T_c \sim (n-n_c)^{w}, \quad w \equiv z\nu, \tag{10}$$

$$T_c \sim [\rho_s(0)]^{x}, \quad x \equiv z/(d+z-2), \tag{11}$$

where $\rho_s(0)$ is the superfluid density at $T=0$. The torsional oscillator experiment discussed below addresses the validity of these scaling laws for ^{4}He films adsorbed in aerogel glass.

1. Heat capacity

We now consider the low-temperature heat capacity on both sides of the onset transition. Technically, the only requirement for the Bose glass is that the excitation spectrum be gapless. This admits almost any power-law dependence of $C(T)$, although for a true glass, i.e., constant density of states, $C(T) \propto T$. On the superfluid side of the onset transition, the dominant low-energy excitations are long-wavelength third sound modes, leading to a Debye specific heat, $C(T) \sim T^d$ for $T \ll T_c$.

At onset $(n=n_c)$, the specific heat can be inferred from the scaling form for the free energy [Eq. (6)]. In order for $f_s(T)$ to remain nonzero and finite at the transition, the tem-

perature dependent part $\tilde{f}(T/\Omega)$ must assume the form

$$\tilde{f}(T/\Omega)=\tilde{f}(T\delta^{-z\nu})\sim(T\delta^{-z\nu})^{(d+z)/z}, \tag{12}$$

since the sum of all the powers of δ in Eq. (6) must equal zero. At onset,

$$C(T)=T\frac{\partial^2 f}{\partial T^2}\sim T^{d/z} \quad (\delta=0,\ T\to 0). \tag{13}$$

Note that if $z=d$, as is believed to be the case for a Bose glass to superfluid transition, $\lim_{T\to 0}C(T)\sim T$ at onset. The temperature dependence at onset is thus the same as in the Bose glass phase.

2. The inert-layer model

Fisher *et al.*[10] demonstrate that in the mean-field limit, their scaling theory reduces to the inert-layer model, in which the superfluid film is taken to coexist with a solidlike ^{4}He underlayer. In this case, exchange between the superfluid film and the localized layer is assumed to be negligible, and the thermodynamics of the system near the onset of superfluidity can be deduced from consideration of an ideal Bose gas coexisting with a solid ^{4}He pseudosubstrate.

The superfluid density in this limit should be proportional to $n-n_c$, where the critical coverage n_c is the density of the solid layer. Thus, $\rho_s(0)\sim(n-n_c)^{\zeta}$, where $\zeta=1$ for both $d=2$ and $d=3$. Two more exponents can be inferred directly from the density dependence of the Bose-Einstein condensation temperature:

$$k_B T_c=\frac{2\pi\hbar^2}{m}\left[\frac{N}{V\zeta(d/2)}\right]^{2/d}, \tag{14}$$

where V is the volume (or area in two dimensions) of the system. Strictly, $T_c=0$ for $d=2$ because of the logarithmic divergence of the zeta function $\zeta(1)$. This divergence can be removed through the introduction of a short-length cutoff which accounts for the finite thickness of the film. We thus find $T_c\sim(n-n_c)^w$ and $T_c\sim[\rho_s(0)]^x$, where $w=x=1$ for $d=2$, and $w=x=2/3$ for $d=3$.

We now propose low-temperature forms of the heat capacity for the inert-layer model. For $n>n_c$, the heat capacity of the *ideal* Bose gas has the limiting behavior $C\sim T^{d/2}$ as $T\to 0$. (The presence of superfluidity requires a Debye contribution $C\propto T^d$, but this vanishes more rapidly than the Bose gas contribution in the limit $T\to 0$.) Since the inert-layer model makes no assumptions about the nonsuperfluid film, it admits essentially any form of the heat capacity for densities $n<n_c$.

3. Summary of the scaling laws

In Table I, we summarize the results of the scaling theory for both the Bose glass and inert-layer models. Four possible cases are considered, corresponding to the Bose glass or inert-layer models in either two or three dimensions. In calculating the exponents from Eqs. (9)–(11) and (13), we have used the result $z=d$ as well as the correlation length inequality $\nu\geqslant 2/d$.[15]

TABLE I. Summary of the asymptotic forms for the superfluid density at $T=0$, $\rho_s(0)$, the superfluid transition temperature T_c, and the heat capacity $C(T)$ in the limits $n\to n_c$ and $T\to 0$. The values given are the relevant exponents for the Bose glass and inert layer models in two and three dimensions.

		Bose glass		Inert layer	
Asymptotic form	Exponent	$d=2$	$d=3$	$d=2$	$d=3$
$\rho_s(0)\sim(n-n_c)^{\zeta}$	ζ	$\geqslant 2$	$\geqslant 8/3$	1	1
$T_c\sim(n-n_c)^w$	w	$\geqslant 2$	$\geqslant 2$	1	1
$T_c\sim[\rho_s(0)]^x$	x	1	3/4	1	2/3
$C\sim T^{\theta_-}(n<n_c)$	θ_-	1	1		
$C\sim T^{\theta_0}(n=n_c)$	θ_0	1	1		
$C\sim T^{\theta_+}(n>n_c)$	θ_+	2	3	1	3/2

III. EXPERIMENTAL DETAILS

Two experiments will be discussed in this paper. The first is a systematic study of the superfluid density of ^{4}He films adsorbed in 91% porosity aerogel glass for temperatures between 10 mK and 200 mK. The second experiment is a high-resolution heat capacity study of ^{4}He films adsorbed in Vycor glass for temperatures from 10 to 200 mK. The heat capacity measurements were conducted for coverages on both sides of the onset transition. Brief accounts of these experiments have been published previously.[16–18]

A. Substrates

Vycor and aerogel are both porous glasses. Vycor[19] is prepared by leaching out one phase of a borosilicate glass after spinodal decomposition. The resulting matrix has a distribution of pore diameters with a maximum at approximately 70 Å and a half width of approximately 20 Å. Aerogel[20] is prepared by kinetic aggregation of silica particles in a gel. After hypercritical drying to remove the solvent, the resulting substrate consists of strands of silica approximately 50–100 Å in diameter. Unlike Vycor, there is no characteristic pore size, but the structure is correlated on length scales up to 600 Å for the sample studied in this work.[4] In spite of the structural differences, the superfluid densities of thin ^{4}He films adsorbed in Vycor and 91% porosity aerogel near T_c are remarkably similar, although the heat capacity singularity at the superfluid transition seen in Vycor does not appear in aerogel.[4] As discussed in Ref. 4, the correlated disorder of the substrate is apparently irrelevant for very thin films of superfluid ^{4}He adsorbed on either substrate, since the superfluid correlation length ξ exceeds all structural length scales.

B. Superfluid density measurements

The superfluid density of ^{4}He films adsorbed in 91% porosity aerogel was measured using the torsional oscillator technique.[21] The experimental cell was the same as that described in Ref. 4, which discusses the experimental aspects of the superfluid density measurements in detail. Several important parameters are listed in Table II. All of the torsional oscillator data in this paper will be presented in terms of the *superfluid period shift* ΔP defined below. These data can be

TABLE II. Torsional oscillator parameters for the ^{4}He-aerogel measurements. Additional details are given in Ref. 4. The substrate velocity is estimated from the cell geometry and the various amplifier gains.

Frequency (Hz)	250
Moment of inertia (g cm^2)	0.34
Cell volume (cm^3)	0.13 ± 0.01
N_2 BET surface Area (m^2)	9.2 ± 0.9
Mass sensitivity (nsec/μg)	0.211
Superfluid mass Sensitivity (nsec/μg)	0.022[a]
Q at 10 mK	1.6×10^6
Maximum substrate Velocity at 10 mK (cm/sec)	2×10^{-2}

converted to a superfluid mass by dividing by the *superfluid mass sensitivity* of the cell, 0.022 nsec/μg.

The measurements under discussion here can be divided into two classes. The first comprises temperature sweeps conducted in a manner identical to that described in Ref. 4. For each ^{4}He coverage, the resonant period P and the amplitude of the torsional oscillator were measured as a function of temperature. To determine the superfluid period shift ΔP, we first subtracted the temperature-dependent background of the empty cell from the raw data. The data above the superfluid transition temperature T_c were fitted to a constant. The period data were then subtracted from this baseline, giving the superfluid period shift $\Delta P(T)$. The period shift at $T=0$, $\Delta P(0)$, was determined by fitting $\Delta P(T)$ to a horizontal line at the lowest temperatures. Uncertainties due to the background subtraction and the fact that our lowest reliable measurements could be made only above 10 mK limited the precision of our $\Delta P(0)$ measurements to about ±0.1 nsec.

The superfluid transition temperature T_c was determined with a typical uncertainty of ±0.2 mK by locating the break in $\Delta P(T)$ at the transition. The most precise way to do this was to drift slowly ($dT/dt\sim0.2-0.3$ mK/h) through the transition while recording the resonant period and amplitude of the torsional oscillator. The result of such a drift measurement for $n=35.7$ μmol/m^2 for which $T_c=38.6\pm0.2$ mK is shown in Fig. 3. These data also show two dips in the amplitude. The large feature, near 38 mK, is certainly a sound resonance since the period, which is measured using a phase-locked loop, shows an s-shaped distortion. The smaller peak, which seems to coincide with the superfluid transition, may be due to a cascade of resonances. We do not know why the resonance associated with the large peak is so prominent, since a simple calculation shows that it does not correspond to a low-order third sound resonance. For the thinnest films, the resonance could be seen even when $\Delta P(T)$ was almost obscured by noise and uncertainties in the background subtraction.

For films with transition temperatures above 50 mK, we could also determine T_c by fitting the period shift data near the transition to a power law $\Delta P(T)=At^{\zeta}$, where

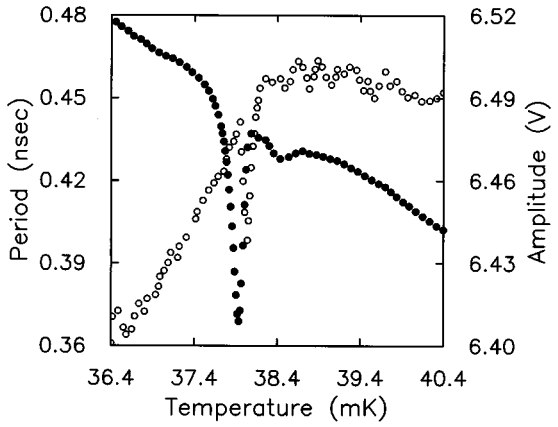

FIG. 3. The resonant period (open circles) and amplitude (solid circles) of the torsional oscillator as a function of temperature during a drift measurement at a coverage of 35.7 μmol/m^2. The period has been offset by $-3.992\,359$ msec.

$t=1-T/T_c$.[4] The T_c determined in this fashion was typically 0.2–0.3 mK below the temperature at which $\Delta P(T)$ was nonzero within the resolution of our measurements. In this sense, the superfluid transition for films on aerogel is considerably sharper than that observed in *rods* of Vycor,[1,13] where a ''foot'' in ρ_s extends 1–2 mK above the superfluid T_c as determined from power-law fits.[22]

C. Heat capacity measurements

The calorimeter, shown in Fig. 4, was constructed from thin-walled silver. Fourteen disks of thickness 0.3–0.6 mm were cut from a slab of Vycor by first coring the slab with a slurry cutter and then slicing off the disks using a diamond-impregnated wire saw. Cutting from a slab with the leaching plane parallel to the surface produces a more homogenous sample than is obtained from rods of Vycor, in which the boron-rich phase is leached from the perimeter.[23] After cutting, the disks were cleaned in hydrogen peroxide and then baked in vacuum. A silver coating, ~0.5 μm thick, was then

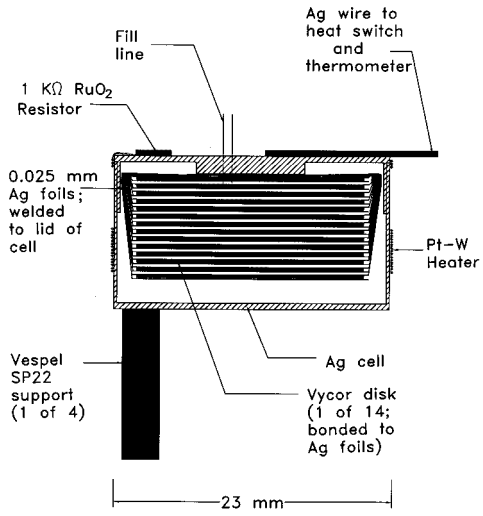

FIG. 4. A cross section of the ^{4}He-Vycor calorimeter. All pieces are made of silver except as indicated.

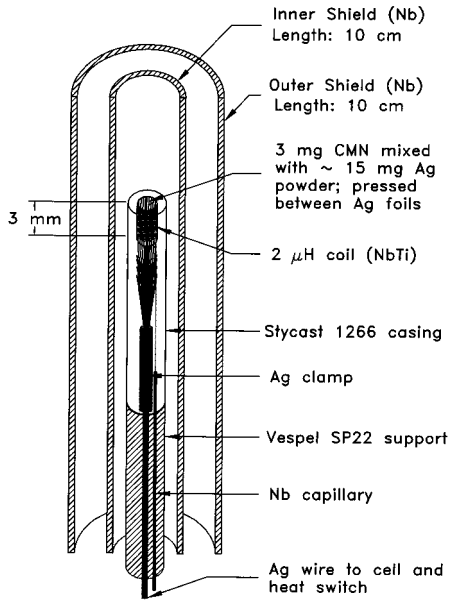

FIG. 5. The CMN magnetization thermometer.

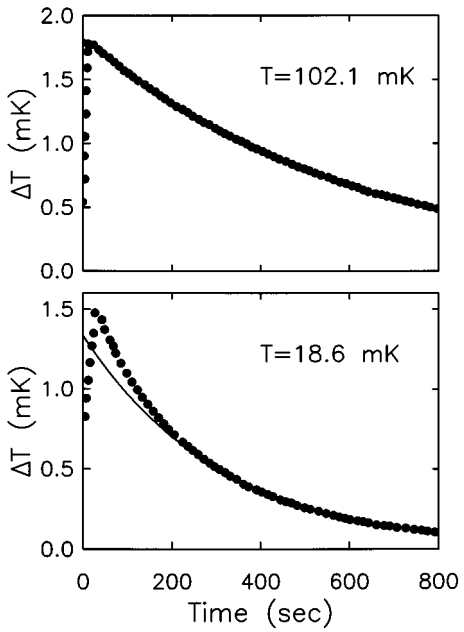

FIG. 6. The response of the calorimeter following heat pulses at 102.1 mK (upper panel) and 18.6 mK (lower panel). The solid curves show exponential fits to the decay curve at long-time scales. Note the deviations at short time scales in the 18.6 mK data.

evaporated on both sides of each disk. The edges were left uncoated to allow the ^{4}He to penetrate the sample. Each disk was then glued to two 0.025 mm thick Ag foils, which had previously been diffusion-welded to the cap of the calorimeter. The calorimeter was sealed with Emerson Cumming Stycast 1266 epoxy. A Pt-W wire heater was wound around the body of the calorimeter, and a 1 kΩ RuO_2 resistor was glued to the cap of the cell. The calorimeter was supported by four Vespel posts and was attached to the low-temperature stage of a $PrNi_5$ demagnetization cryostat. The thermal contact to the stage was controlled using a tin-wire superconducting heat switch.

A low thermal mass dc magnetization thermometer, shown in Fig. 5, was essential for measurements below 20 mK. The actual sensor in this thermometer is a miniaturized version of the design of Greywall and Busch.[24] 2.5 mg of cerous magnesium nitrate (CMN) powder, consisting of grains less than 75 μm in diameter, was mixed with an equal volume of 2–4 μm silver powder and then pressed between 11 0.025 mm thick silver foils. Before pressing with the powder, the foils were annealed, perforated to enhance the adhesion of the Ag-CMN powder, and their ends were diffusion-welded together. After pressing, the assembly was potted in Stycast 1266 epoxy and machined into a cylinder 3 mm in diameter. A 2 μH NbTi wire coil, which was part of a superconducting flux transformer, was then wound around the cylinder, and the foils were attached to an Ag wire using a crimp joint. This assembly was then repotted in epoxy and glued to a Vespel post, which was attached to the low-temperature stage of the refrigerator. Two Nb shields were used to trap a small (25–50 G) magnetic field and for magnetic shielding. The wires for the flux transformer were twisted and then threaded through a Nb capillary to a junction box on the still of the dilution refrigerator. The capillary was filled with silicon oil in order to prevent any vibrations of the twisted pair. The remainder of the flux transformer passed through a feedthrough into the bath space and was attached to the input coil of a commercial dc SQUID.[25]

The operation of the thermometer is identical in principle to the high-resolution thermometer developed for λ-point experiments by Lipa and Chui.[26] Some details have been published previously by our group.[21] The magnetization is measured by monitoring the current in the flux transformer, which changes so as to keep the total flux enclosed by the superconducting loop constant. The sensitivity of the thermometer is determined by the applied field. The price paid for the sensitivity of the dc magnetization thermometer is the need to count flux, since the dynamic range of the flux-locked loop is limited, and so the loop must therefore be reset periodically. In practice, we regularly exceeded the slew rate of the SQUID electronics and the flux count therefore became meaningless. This inconvenience was ameliorated in our case by the availability of the heat switch on the calorimeter, which could be closed to check the magnetic thermometer against a ^{3}He melting curve thermometer on the stage at any point during the experiment.

The heat capacity measurements were conducted using the adiabatic calorimetry technique. A current pulse was applied to the heater, and the resulting thermal response of the cell was recorded. Two response curves, recorded at temperatures of 102.1 and 18.6 mK for a coverage of 27.1 μmol/m^2, are shown in Fig. 6. These data are representative of two classes of response curves that we found. Above 80 mK, the temperature of the cell decayed exponentially after the pulse, and the temperature step ΔT was determined simply by extrapolating the exponential decay back to the midpoint of the heat pulse. At lower temperatures, the decay became nonexponential, as can be seen in the lower panel of Fig. 6. Since we could fit the long-time part of the decay to an exponential, we first believed that the short-time behavior reflected a thermal overshoot due to poor thermal contact between the ^{4}He film and the calorimeter. If we extrapolated

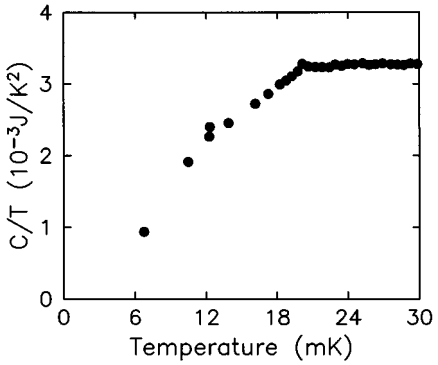

FIG. 7. Heat capacity, divided by temperature, for a coverage of 27.6 μmol/m^2 of ^{4}He on Vycor. The cusp at 20 mK is a signature of the superfluid transition.

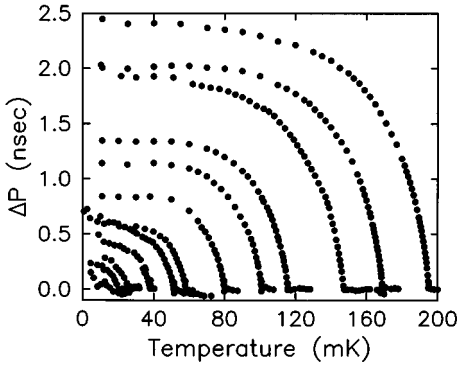

FIG. 8. The superfluid period shift ΔP as a function of temperature for 12 coverages of ^{4}He adsorbed on 91% porosity aerogel glass.

the long-time behavior back to the midpoint of the pulse, however, the inferred heat capacities were clearly too high. This suggested that either heat was leaking out of the calorimeter on short-time scales, hence leading to an overestimate of the heat capacity, or that the anomalous decay was due to some internal relaxation mechanism, perhaps reflecting a significant heat capacity in poor thermal contact with the rest of the calorimeter. The former possibility was unlikely since the superconducting heat switch provides its best thermal isolation at the lowest temperatures. We suspected that the Vycor itself might harbor a thermal reservoir and modeled the thermal relaxation inside the cell assuming the existence of a reservoir that was weakly linked to the ^{4}He film.[17] This provided a reasonable fit to the decays, but we found that the thermal conductivity to the weakly linked reservoir depended on both coverage and temperature. A similar coverage-dependent coupling between the ^{4}He film and the Vycor itself has been observed in ultrasound measurements.[27] We decided to proceed on the assumption that the ^{4}He film equilibrated rapidly with the thermometers, in which case the temperature step ΔT for determining the specific heat should be extracted from the response of the calorimeter at short-time scales. We tested this hypothesis by dosing approximately 2 monolayers of ^{3}He into the calorimeter at the end of the run. This film had a heat capacity approximately 60 times larger than any of the ^{4}He films in our experiment. The ^{3}He film equilibrated within 120 sec after each heat pulse, justifying our assumption about the short-time scale behavior of the calorimeter at low temperatures.

The heat capacity for a coverage of 27.6 μmol/m^2 is shown in Fig. 7 after dividing by the temperature T. These data, taken with the magnetization thermometer, show a cusp at 20 mK, which is a signature of the superfluid transition.[28,29] (Since we did not take a BET isotherm for this sample, the surface area was determined by comparing our measured superfluid transition temperatures as a function of ^{4}He dosage with those of Crooker *et al.*[13]) The ordinary low-temperature limit of our measurements was 10 mK. This was determined by the internal heat leak of the calorimeter, which decayed from approximately 0.8 to 0.4 nW over the course of 3 months. This large heat leak, which we suspect was due to the Vycor in the calorimeter, required us to run with the heat switch partially open at the lowest temperatures. Obtaining a proper tuning of the heat switch was very tedious, and this turned out to be the primary impediment to using the calorimeter below 10 mK.

IV. RESULTS

A. Superfluid density

In Fig. 8, we show the period shift data for 12 coverages of ^{4}He adsorbed on aerogel. The superfluid period shift at $T=0$, $\Delta P(0)$, was obtained by fitting the low-temperature part of each curve to a horizontal line. The transition temperature T_c was determined for each coverage using the drift technique described above. In Fig. 9, we show T_c and $\Delta P(0)$ as a function of coverage. The curves show fits to power laws

$$T_c(n)=T_0(n/n_c-1)^w \tag{15}$$

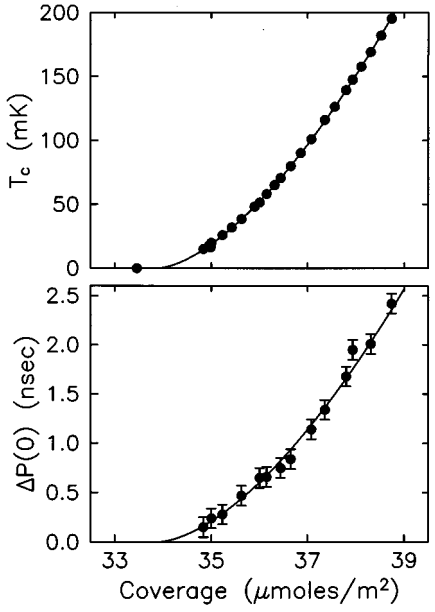

FIG. 9. The superfluid transition temperature T_c and the period shift at $T=0$, $\Delta P(0)$, as a function of the the ^{4}He coverage for films adsorbed in aerogel. The solid curves are fits to the power laws of Eqs. (15) and (16).

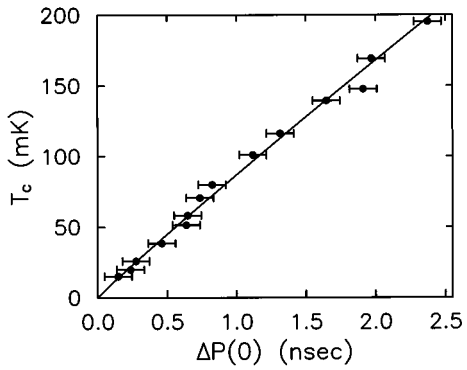

FIG. 10. The superfluid transition temperature T_c as a function of the period shift at $T=0$, $\Delta P(0)$. The solid curve is a fit to Eq. (17).

and

$$\Delta P(0)=D_0(n/n_c-1)^{\zeta}, \tag{16}$$

where we find $w=1.59\pm0.06$ and $\zeta=1.64\pm0.04$. The critical coverage $n_c=33.89\pm0.08$ μmol/m^2 was determined from the fit of T_c versus coverage and then held fixed for the fit of the period shift data. The final relation of interest is the dependence of T_c on $\Delta P(0)$, which is shown in Fig. 10. In this case, we have fitted the data to the power law

$$T_c=A[\Delta P(0)]^x, \tag{17}$$

where we find $x=0.95\pm0.02$. The measured exponents are listed in Table III along with corresponding values we obtain from fits of the data of Crooker[30] for the ^{4}He-Vycor system.

We will discuss the exponents of Table III in more detail below. Another point of interest is the size of the ''critical region'' for the onset transition. Since the fits of the various power laws are poor (by the standards generally applied to critical phenomena), the usual practice of looking at deviations from the power-law behavior is not particularly instructive. Another approach is simply to see how the data near onset compare with those further away from the transition. We do this for $\Delta P(0)$ as a function of coverage in Fig. 11. The highest coverage in this figure has a T_c of approximately 1 K. A significant departure from linear behavior is seen only for films with $\Delta P(0)<1.5$ nsec, or $T_c<150$ mK. The linear dependence of $\Delta P(0)$ on n at higher coverages is consistent with the inert-layer model of the onset transition, so the data of Fig. 11 indicate only a small coverage regime in which fluctuations associated with the onset transition might be relevant. The evolution of T_c with $\Delta P(0)$ is even more striking in this regard, since, as shown in Fig. 12, the nearly linear behavior observed for thin films continues for films with

TABLE III. Experimental values of the exponents ζ, x, and w for aerogel and Vycor. The Vycor exponents are based on fits to the data of Crooker (Ref. 30).

Exponent	Aerogel	Vycor
ζ	1.64 ± 0.04	2.5 ± 0.3
x	0.95 ± 0.02	0.85 ± 0.02
w	1.59 ± 0.06	1.76 ± 0.01

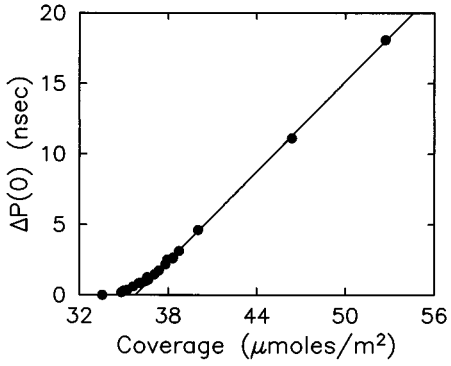

FIG. 11. $\Delta P(0)$ as a function of the ^{4}He coverage for films with transition temperatures up to 1 K. The solid curve is a linear fit to the data for films with T_c's greater than 150 mK.

T_c's up to 0.7 K. [This linear dependence is suggestive of the Kosterlitz-Thouless-Nelson (KTN) relation for a two-dimensional superfluid,[31] for which $\rho_s(T_c^-)/T_c=8.73$ μmol m^{-2} K^{-1}, where $\rho_s(T_c^-)$ is the limiting superfluid density as the transition temperature is approached from below. For reasons of comparison in Fig. 12, we have converted the period shift to *areal superfluid density* using the calibration $\rho_s/\Delta P=1.24$ μmol m^{-2} nsec^{-1}. The slope of the KTN line, which is drawn dashed in the figure, is about twice that of a linear fit to the data of Fig. 12. Although we expect $\rho_s(T_c^-)$ to be reduced from $\rho_s(0)$ by elementary excitations and vortex pair screening, the discrepancy between the two slopes is not resolved in a full fit of the superfluid density data to the finite size theory[32] for a superfluid film adsorbed on a cylindrical strand. The best-fit coverage for each data set that is about half the actual coverage.[33] We do not believe, however, that the failure of this naive application of the KTN relation says anything about the effective dimensionality of the film, which will be discussed further below.]

B. Heat capacity

The ^{4}He-Vycor heat capacity data, divided by temperature, are shown for ten coverages in Fig. 13. Each of the data

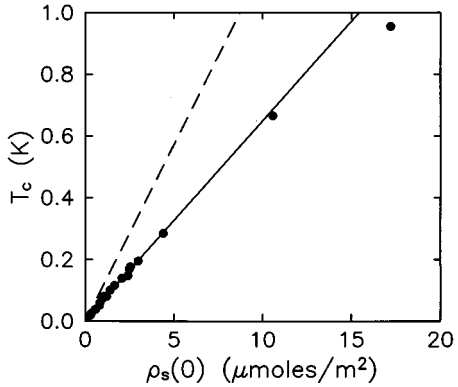

FIG. 12. The superfluid transition temperature T_c as a function of the areal superfluid density at $T=0$, $\rho_s(0)$ for films with transition temperatures up to 1 K. The solid curve is a linear fit to the data for films with $T_c<300$ mK. The dashed curve is the KTN line $\rho_s(T_c^-)/T_c=8.73$ μmol m^{-2} K^{-1}.

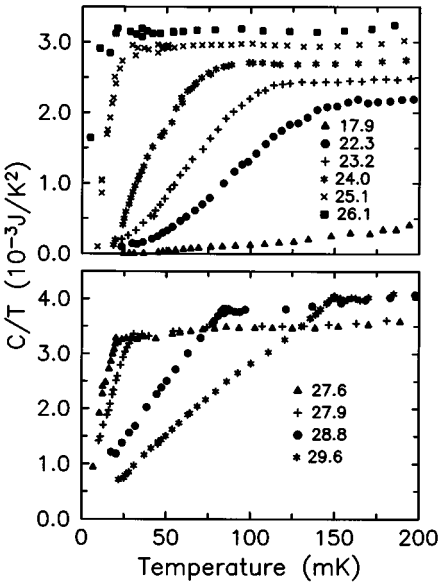

FIG. 13. The heat capacity, divided by temperature, is shown as a function of temperature for 10 coverages of ^{4}He adsorbed on Vycor glass. The coverages in μmol/m^2 are given in the legend. Nonsuperfluid coverages are shown in the upper panel and superfluid coverages are shown in the lower panel.

sets in the lower panel of the figure shows a sharp cusp, corresponding to a superfluid transition.[28] The superfluid transition temperatures determined from the locations of the cusps are shown as closed circles in Fig. 14. The critical coverage n_c for the onset of superfluidity is determined by extrapolating the T_c data to zero temperature. For temperatures $T<T_c$, the heat capacity of the superfluid films is roughly quadratic in temperature, while it depends nearly linearly on temperature for $T>T_c$, with a small quadratic correction that increases with coverage. In the vicinity of the superfluid transition, there is a small peak in C/T due to critical fluctuations.[28,29] The size of the peak decreases with decreasing thickness. As can be seen in Fig. 7, this peak can barely be resolved for the thinnest superfluid film ($T_c = 20.5$ mK).

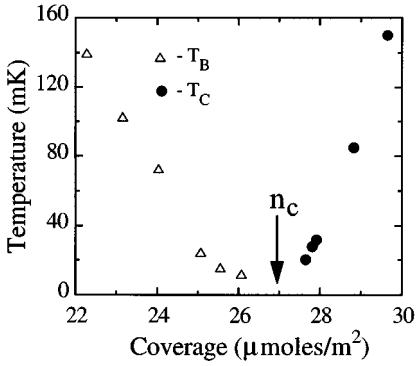

FIG. 14. The superfluid transition temperature T_c (circles) and the crossover temperature T_B (triangles) defined in the text are shown as a function of coverage for ^{4}He on Vycor. The onset coverage n_c determined by extrapolating the T_c data is indicated with the arrow.

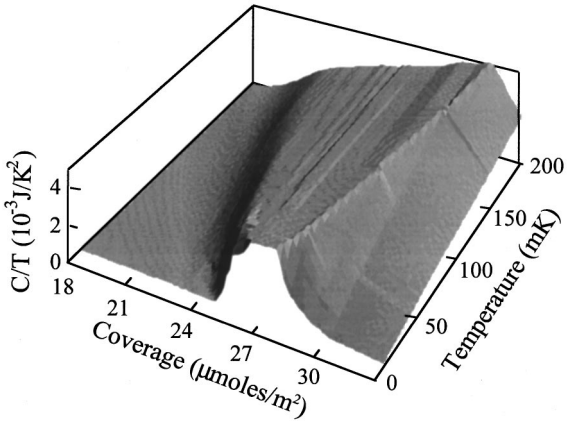

FIG. 15. A three-dimensional representation of the C/T data for ^{4}He in Vycor for $T<200$ mK over the coverage range of our experiment.

At high temperatures, the heat capacity of nonsuperfluid films, shown divided by temperature in the upper panel of Fig. 13, depends linearly on temperature, but C/T drops rapidly at low temperatures. We define a crossover temperature T_B separating these two regimes to be the point at which C/T is half of its high-temperature value. T_B is shown as a function of coverage in Fig. 14, along with the T_c's measured for the superfluid films. This plot shows clearly that T_B vanishes as the onset transition is approached from below. (Although our definition of T_B is somewhat arbitrary, any reasonable choice of a characteristic temperature for the crossover would show the same coverage dependence.) For $T>2T_B$, there is not much qualitative difference between the heat capacity of a nonsuperfluid film and that of a superfluid film for $T>T_c$. This is emphasized in the three-dimensional representation of our data shown in Fig. 15, in which there is a wedge-shaped plateau in the vicinity of the onset coverage $n_c=27$ μmol/m^2. Above 20 mK, the heat capacity isotherms, which are cross sections of the 3D surface, show no feature at n_c. The peaks in the isotherms become progressively narrower in coverage as the temperature is reduced, but we cannot reliably extrapolate our data to $T=0$.

V. DISCUSSION

The data introduced above indicate that the concept of a superfluid-insulator transition in ^{4}He films is qualitatively appropriate. Both sets of measurements indicate the existence of a critical coverage n_c at which the superfluid transition temperature T_c vanishes. The heat capacity data are particularly instructive in this regard, since there is a characteristic energy k_BT_B for nonsuperfluid films which also vanishes as n_c is approached from *below* in coverage.

A. Scaling theory

1. ρ_s measurements

As can be seen by comparing the exponents of Table III with the predictions of Table I, the experimentally determined exponents for the onset transition are not consistent with the scaling theory for either $d=2$ or $d=3$. We have

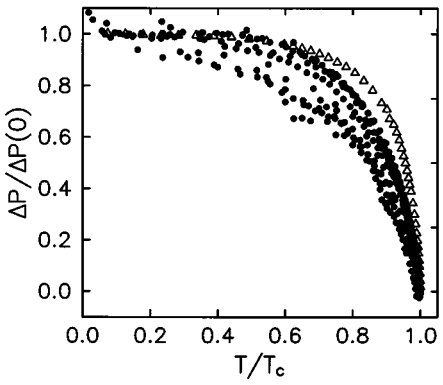

FIG. 16. The period shift data for coverages of ^{4}He in aerogel with the period shift scaled by $\Delta P(0)$ and the temperature scaled by T_c. Open triangles correspond to a coverage of 52.7 μmol/m^2, for which $T_c = 955$ mK. These data were obtained during a separate run. All solid circles are for coverages with $T_c < 200$ mK. The lowest coverage in this figure is 35.2 μmol/m^2, for which $T_c = 26$ mK.

also seen in Figs. 11 and 12 that the departure from the behavior seen at higher coverages ($T_c > 200$ mK) is actually quite small. Some curvature is apparent in $\Delta P(0)$ at the lowest coverages, but the relation between T_c and $\Delta P(0)$ remains nearly linear for T_c's from 700 mK down to the lowest T_c in our study (20 mK). These observations lead us to question whether our measurements are in the asymptotic regime of reduced coverage $n - n_c$ in which the scaling theory is valid. To address this question, we return to the asymptotic form of the free energy, Eq. (6). This scaling form comprises the product of the free energy at $T = 0$ and a function of $T/\Omega = u_c T/T_c$. This implies

$$\frac{\rho_s(T)}{\rho_s(0)} \sim \tilde{u}(u_c T/T_c) \tag{18}$$

in the asymptotic regime, where $\tilde{u}$ is a universal function. Thus, upon scaling the period shift ΔP by $\Delta P(0)$ and the temperature by T_c, all of the $\Delta P(T)$ data in the asymptotic regime should collapse on to a universal curve. As can be seen in Fig. 16, our data do not scale in this fashion. In fact, the scaled data in this figure drift continuously toward the origin as the coverage is reduced. There is no indication that the data are even approaching a universal curve. The scaling plot demonstrates explicitly that the properties of superfluid films at nonzero temperature are *not* determined by the single energy scale Ω. Therefore, we should not expect the scaling laws [Eqs. (10) and (11)] for T_c as a function of n or $\rho_s(0)$ to hold in the coverage range of our experiment.

Although we have shown explicitly that the scaling theory does not hold at nonzero temperature (i.e., $T > 20$ mK), we must still consider the possibility that it holds at $T = 0$. Only one of the scaling laws, $\rho_s(0) \sim (n - n_c)^{\zeta}$, applies in this case, but the experimental result $\zeta = 1.64 \pm 0.04$ is well below the theoretical bounds $\zeta \geqslant 8/3$ for $d = 3$ or $\zeta \geqslant 2$ for $d = 2$. Since, as shown in Fig. 11, the data approach the inert-layer prediction at higher coverages, it is reasonable to ask if our low-coverage data fall in a crossover regime in which quantum fluctuations are relevant but not yet dominant. This is certainly possible, but it leads one to ask why the critical region in coverage should be so small. In order to address this question, we convert the coverage to the chemical potential μ using the van der Waals relation

$$\mu(n) = -\frac{\alpha}{n^3}, \tag{19}$$

where $\alpha = 27$ K (layer)^3 for ^{4}He on glass.[34] Although the chemical potential is difficult to measure in this coverage range, third sound measurements, which determine $\mu(n)$ indirectly, are consistent with the form of Eq. (19).[1] Assuming a monolayer coverage of 13 μmol/m^2, $n_c \approx 2.6$ layers for ^{4}He-aerogel and $n \approx 3.0$ layers for a film with a T_c of 200 mK. The chemical potential thus shifts from about -1.5 K at onset to approximately -1.0 K for films with T_c's near 200 mK. Given that the characteristic exchange energy for the ^{4}He films is on the order of 1–2 K,[35] a chemical potential shift of 0.5 K cannot be considered small.

The rapid change of μ with coverage also leads to a technical problem in applying the scaling theory: the assumption $n - n_c \sim \mu - \mu_c$ is not correct, even in the narrow coverage range of our experiment. Assuming that μ follows the form of Eq. (19), we have converted coverage to chemical potential and have fitted our data to the power law

$$\Delta P(0) \sim (\mu - \mu_c)^{\zeta}. \tag{20}$$

In effect, this allows us to eliminate the assumptions implicit in Eq. (8), with the caveat that we have not actually measured the chemical potential. We find an exponent $\zeta = 2.2 \pm 0.1$ by this approach. The case for the Bose glass is thus improved in $d = 2$, although the inequality of Eq. (9) is still not satisfied for $d = 3$. We note, however, that the theory cannot be applied self-consistently in $d = 2$, since it assumes a diverging correlation length which will eventually exceed the strand size of the aerogel. In this case, topological arguments lead us to expect that the onset transition must be three-dimensional in character, although we cannot exclude the possibility of an observable crossover regime between 2D and 3D behavior.

We thus find that two conditions of the scaling theory do not apply in the case of ^{4}He adsorbed in aerogel in the coverage range of our study. First, there is no single energy scale that determines the thermodynamic properties at finite temperature. Second, the chemical potential changes rapidly with coverage, which makes the asymptotic regime difficult to achieve and also implies that the reduced density $n - n_c$ is not simply proportional to $\mu - \mu_c$. We recall at this point the third (and most fundamental) assumption of the theory, which is that the nonsuperfluid phase is compressible. (This assumption is critical to establishing the relation $z = d$ for the dynamic exponent.) Since the compressibility is given by $\partial n/\partial \mu$, Eq. (19) suggests that although κ will be nonzero, it will be considerably lower than for an idealized ^{4}He film such as that considered in the Bose-Hubbard model.[10–12] In effect, the adsorption potential adds a third energy scale to the problem in addition to the exchange energy and the interparticle repulsion. The strong binding to the substrate makes the film much less compressible than it would be if it were ''free-standing.''[36] Even if κ is technically nonzero, the film may be sufficiently incompressible that the softening due to quantum fluctuations is negligible.

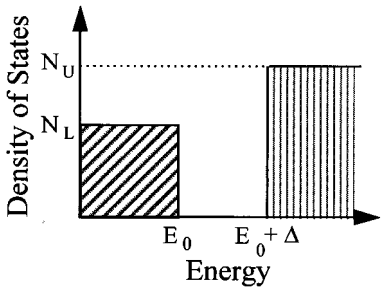

FIG. 17. A model single-particle density of states for nonsuperfluid ^{4}He films adsorbed in Vycor (Ref. 37). The states below E_0 are localized, and the states above $E_0+\Delta$ are extended.

2. C(T) measurements

The heat capacity measurements allow us to test the predictions of the scaling theory below the onset of superfluidity. As shown in Fig. 13, the salient feature of $C(T)$ for coverages below onset is a characteristic temperature T_B below which C/T drops rapidly to zero and above which it approaches a constant. As shown in Fig. 14, T_B vanishes as the onset of superfluidity is approached from below. At the onset transition, $C(T)$ is approximately linear over the entire temperature range, $T>10$ mK, covered by our experiment.

The fact that $C(T)$ is linear in T for $n=n_c$ is in apparent agreement with the scaling theory of Fisher *et al.*[10] (see Table I). Below onset, however, the data show only a single region of linear behavior, although the Bose glass model predicts two regions: one at low temperature due to the Bose glass and a second at higher temperatures due to quantum fluctuations. One possible explanation for the single linear region is that the Bose glass contribution is immeasurably small. This would be consistent with the observation made above that the strong van der Waals potential makes the ^{4}He film nearly incompressible.

Assuming for the moment that the Bose glass contribution to the heat capacity is too small to be measured, we turn to the linear behavior that we do observe. At onset this is predicted by the scaling theory of Fisher *et al.*, in which the contribution to C from quantum fluctuations varies linearly with temperature. We note, however, that the linear behavior is observed over a very wide temperature range, extending up to at least 600 mK, while the superfluid density data for both aerogel and Vycor indicate that the critical regime in which quantum fluctuations are relevant is confined to coverages with T_c's less than 200 mK. Although there is no reason why the asymptotic critical regions observed for two different thermodynamic quantities must be the same, it would be rather unusual to see critical behavior so readily in $C(T)$ when all other measurements suggest that the critical regime is nearly inaccessible.

B. Activation model for nonsuperfluid films

As can be seen in Fig. 13, the heat capacity of nonsuperfluid films drops off very rapidly, faster than T^3, at low temperatures. This behavior is suggestive of a gap in the excitation spectrum of the film. The simplest density of states that includes a gap is shown in Fig. 17. The model, considered originally by Tait and Reppy,[37] includes two bands of states.

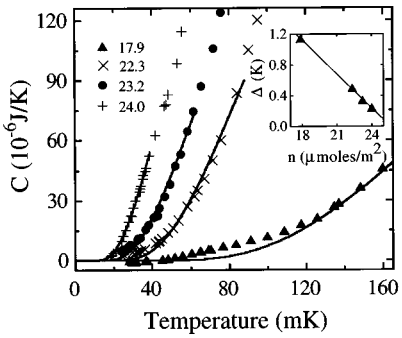

FIG. 18. Low-temperature heat capacity data for nonsuperfluid coverages of ^{4}He in Vycor. The solid curves are fits to the activation model discussed in the text. The coverages in μmol/m^2 are indicated in the legend. The inset shows the gap [see Eq. (21)] as a function of the coverage.

The lower band comprises localized states due to the heterogeneous adsorption potential. Because of the strong repulsive He-He interactions, each localized state can accommodate only a single He atom, leading to effective Fermi statistics in the lower band of Fig. 17. The upper band, which is unoccupied at $T=0$, consists of extended states, which are assumed to obey Bose statistics at low densities. This model leads to a heat capacity of the form

$$C=D(\Delta/2k_BT+2)e^{-\Delta/2k_BT} \tag{21}$$

for $k_BT\ll\Delta$. The prefactor $D=\sqrt{N_lN_u}\Delta k_B$, where N_l and N_u are the densities of states in the lower and upper bands. The results of fits to Eq. (21) for four nonsuperfluid films in the regime $T<T_B$ are shown in Fig. 18. The gap Δ is shown as a function of coverage in the inset. For each coverage, we find a gap of order $5T_B$.

Our data are not precise enough to distinguish between a true gap in the density of states and a ''soft gap,'' in which a low-energy tail exists in the band of extended states. It is possible that a small number of extended states exist at energies well below Δ. In principle, it would be possible to place a bound on the number of such states by determining how much of the classical entropy is *not* frozen out at low temperatures. Unfortunately, this calculation is impossible because our data do not reach a limit in which $C(T)$ is independent of temperature. (This limit could not be reached without macroscopically populating the vapor phase, which is ignored in our model.)

There is no *a priori* reason for our having chosen a *constant* density of states in each of the bands shown in Fig. 17. As far as fitting the data of Fig. 18 is concerned, the critical element of the excitation spectrum is the gap. Additional information, however, comes from the high-temperature data on both sides of the onset transition. In both cases, the heat capacity depends linearly on temperature in this regime. For $n<n_c$, only the extended states contribute to the heat capacity at high temperature, and a linear temperature dependence would follow from a constant density of states. The only difference for superfluid films ($n>n_c$) is that some extended states are occupied at $T=0$. For $T>T_c$ we would expect to see the same temperature dependence as observed for films below the critical coverage. Based on Fig. 15, this appears to

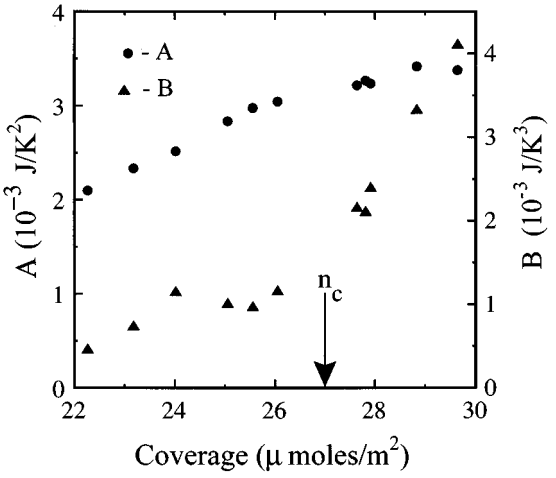

FIG. 19. The coefficients A (circles) and B (triangles) in fits of the high-temperature ($T>T_c$ or $T>2T_B$) heat capacity data to the form $C(T)=AT+BT^2$. The arrow indicates the onset coverage n_c.

be the case, since the wedge-shaped plateau at high temperatures extends to both sides of the critical coverage. We have also fitted the high-temperature ($T>2T_B$ or $T>T_c$) data to the form $C(T)=AT+BT^2$ on both sides of the onset transition. As can be seen in Fig. 19, the linear coefficient A increases slowly with coverage, with no apparent feature at the onset transition, which is marked in the figure by the arrow. The quadratic contribution, however, increases rapidly for coverages above onset, although it remains at least a factor of two smaller than the linear heat capacity for $T<400$ mK.

The onset of superfluidity in ^{4}He films adsorbed in Vycor thus corresponds to the closing of a gap in the excitation spectrum of the film as the coverage is increased. Although this is a Bose insulator to superfluid transition, the insulating phase is not gapless, in disagreement with the assumptions of the Bose glass model. Although this conclusion turns to some degree on whether or not we can resolve a small but nonzero density of states at low temperatures, there is also a significant philosophical distinction between the activation model we have employed here and the Bose glass approach. In the Bose glass model, superfluidity is destroyed at $n=n_c$ by order parameter phase fluctuations. The Bose condensate (essentially the microscopic order parameter) is assumed to exist below onset, even though long-range order does not. In the simple activation model employed here, there is no order parameter below onset, since none of the extended states in the system are occupied at $T=0$. A similar distinction appears for the case of the superconductor-insulator transition, for which two classes of transitions have been observed. For granular films, the order parameter is nonzero at the superconductor-insulator transition,[38] and the superconductor-insulator transition is driven by fluctuations in the phase of the order parameter. There is also evidence for a Bose glass phase in some homogeneously disordered films,[39] but other experiments suggest that the amplitude of the order parameter vanishes at the superconductor-insulator transition in this case.[40] At the moment, we cannot probe the microscopic order parameter in our system, and so we cannot determine directly whether or not a condensate exists for coverages below the onset of superfluidity.

C. Thin superfluid films

As discussed above, the rapid change of the chemical potential μ with coverage near n_c tends to make quantum fluctuations less important in ^{4}He films than they would be if the adsorption energy were less strongly dependent on coverage. The large spread in energy scales due to the adsorption potential minimizes exchange between atoms in the localized layer and those in the overlying superfluid film. We believe this lies behind the qualitative success of the inert layer model for thicker films, and it is reasonable to ask how close to the onset transition one can neglect exchange with the nonsuperfluid film.

If we ignore the ^{4}He atoms in the localized layer in our aerogel sample, we estimate that the interparticle spacing d for the atoms in the superfluid film is at least 10 Å for $T_c<80$ mK. This estimate follows from dividing the number of superfluid atoms by the *surface area* (9.2 m^2) of the substrate. Estimates based on the total *volume* occupied by the substrate (0.13 cm^2) give an interparticle spacing on the order of 30 Å for a film with $T_c=80$ mK.[41] Both of these estimates indicate that it is not unreasonable to look for dilute Bose-gas-like behavior, since the s-wave scattering length characterizing the He-He interaction is of order 3 Å.

A full formalism for the crossover from a strongly interacting superfluid to a dilute Bose gas as the ^{4}He coverage is reduced has been developed by Weichman and co-workers.[42] The starting point for this theory is the observation that thin films of ^{4}He adsorbed on Vycor show 3D XY critical behavior for coverages with transition temperatures above 120 mK.[1] Identical critical behavior (for films with T_c's down 50 mK) has been observed in ^{4}He films adsorbed in 91% porosity aerogel glass.[4] In both systems, power-law behavior of the superfluid density is observed over at least one order of magnitude in reduced temperature. Weichman *et al.* derive a scaling function which in principle can be used to test for crossover from conventional 3D XY critical behavior to dilute Bose gas behavior as the ^{4}He density decreases. The scaling function reduces to the dilute Bose gas form $\rho_s(T)\sim\rho_s(0)[1-(T/T_c)^{3/2}]$ as $T\to 0$ and to the 3D XY model form $\rho_s(T)\sim\rho_{s_0}(1-T/T_c)^{\zeta}$ ($\zeta\approx 2/3$) as $T\to T_c$. Physically, the scaling function accounts for the reduction in the size of the 3D XY critical regime as T_c decreases. Unfortunately, the Bose gas and 3D XY limits are sufficiently distinct that a scaling function capable of accounting for the crossover can be used to collapse data from essentially any superfluid film.[2] The two limiting forms, however, suggest another way of testing for crossover to Bose gas-like behavior.[13] The quantity $\lim_{T\to T_c}\rho_s(T)/(T_c-T)$ *diverges* in the strongly interacting limit but remains finite for the dilute Bose gas. In Fig. 20, we plot $\Delta P(T)/(T_c-T)$ as a function of T/T_c for four coverages of ^{4}He adsorbed on aerogel. The dilute Bose gas prediction [assuming the same ratio $\Delta P(0)/T_c=12$ psec/mK found for the four films] is shown as a dash-dotted line. The divergence near T_c is pronounced for all of the films.

There is thus no convincing evidence that ^{4}He films adsorbed in aerogel approach Bose-gas-like behavior for films

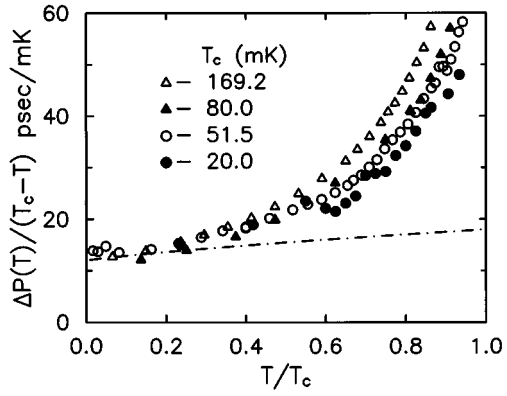

FIG. 20. Period shift data for four coverages, scaled as described in the text, compared with the predictions for a dilute Bose gas. The Bose gas prediction is shown as a dash-dotted line for the case $\Delta P(0)/T_c = 12$ psec/mK. The transition temperatures for each of the data sets are indicated in the legend.

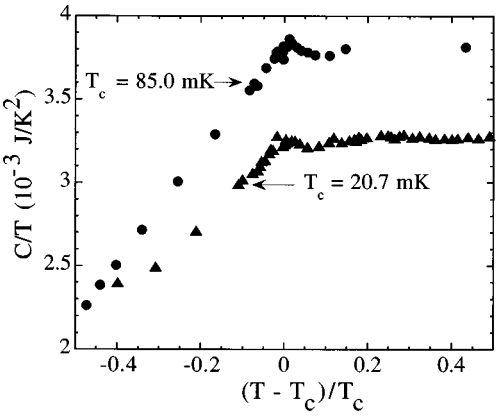

FIG. 21. The heat capacity divided by temperature shown as a function of the reduced temperature $(T-T_c)/T_c$ for coverages of 28.8 μmol/m^2 ($T_c = 85.0$ mK) and 27.6 μmol/m^2 ($T_c = 20.7$ mK).

with T_c's down to 20 mK. The absence of any observable crossover may be due to exchange with the localized layer or simply the possibility that our films were not sufficiently dilute. Crooker *et al.* studied films with T_c's down to 7 mK in their study of the ^{4}He-Vycor system and found a progressive decrease in the 3D XY critical regime as determined from the same analysis used here to produce Fig. 20. Unfortunately, the superfluid signal for a given substrate volume is smaller for aerogel than for Vycor, and the thermal time constants are much longer in aerogel, so extending our measurements to lower coverages and temperatures would not be a trivial task. This is unfortunate, since the superfluid transitions in ^{4}He-aerogel are ''sharper'' than those in ^{4}He-Vycor, in the sense that ρ_s goes to zero only 0.2–0.3 mK above T_c (as determined from power-law fits[4]) as opposed to 1–2 mK in Vycor. Kotsubo and Williams[2] have noted that the smearing of the transition in the Vycor case tends to mimic crossover to Bose-gas-like behavior. There is now convincing evidence that the 1–2 mK ''foot'' in the Vycor data was due to macroscopic inhomogeneities introduced by the leaching process used to produce the porous glass.[23] A new Vycor study, with more homogeneous samples, would probably be much more conclusive than the experiment of Crooker *et al.* in testing for crossover to dilute Bose gas behavior. Porous gold substrates,[43] which recent full-pore measurements suggest are as homogeneous as Vycor, could be an even better substrate for ultra-low-temperature measurements.

The difficulties in interpreting the ρ_s measurements for very thin superfluid films have been compounded by the absence of a complementary study of other thermodynamic quantities in this coverage regime. Our heat capacity measurements for ^{4}He-Vycor begin to address this problem, although the lowest transition temperature we were able to achieve was only 21 mK, significantly higher than the lowest T_c ($\sim$7 mK) reached in the ρ_s study of Crooker *et al.*[13]

In Fig. 21, we show heat capacity data for two superfluid coverages, $n = 28.8$ μmol/m^2 ($T_c = 85$ mK) and $n = 27.6$ μmol/m^2 ($T_c = 20.7$ mK). The heat capacity is divided by temperature and is plotted as a function of the reduced temperature $(T-T_c)/T_c$. The heat capacity for both coverages crosses over from a predominantly linear dependence on temperature above T_c to a quadratic dependence for $T<T_c$. In addition to these ''backgrounds,'' there is a peak in the upper data set ($T_c = 85$ mK) at the transition. A peak can only barely be resolved for the film with $T_c = 20.7$ mK. This trend is consistent with that observed in earlier studies,[28,29] in which the magnitude of the heat capacity peak for ^{4}He films adsorbed in Vycor was shown to scale according to the hyperuniversality relation,[44]

$$\frac{C_s'(t)}{C_s(t)} = \frac{\xi(t)^3}{\xi'(t)^3}, \tag{22}$$

for two systems, denoted primed and unprimed, within the same universality class. In Eq. (22), t is the reduced temperature $(T_c-T)/T_c$ and ξ is the correlation length. Correlation lengths for the ^{4}He-Vycor system can be estimated from the Josephson relation,[45]

$$\xi(t) = \left(\frac{k_B T m^2}{\hbar^2}\right)\frac{1}{\rho_s(t)}, \tag{23}$$

and ρ_s data from the studies of Bishop *et al.*[1] and Crooker *et al.*[13,30] Based on these studies, we estimate that the correlation length for a given reduced temperature will be approximately twice as large for the film with $T_c = 20.7$ mK than for the film with $T_c = 85$ mK.[30] According to the hyperuniversality relation Eq. (22), the heat capacity peak for the thinner film should therefore be eight times smaller than for the thicker film, which is consistent with Fig. 21.

A rigorous test of Eq. (22) for ^{4}He films in Vycor would require fitting each of the heat capacity data sets to power laws near T_c. This is impractical at the moment due to both the noise in the data and the ambiguities in subtracting a nonsingular background. Although the noise could be reduced in a better experiment, the interpretation of the background heat capacity poses a more fundamental problem. In Fig. 21, the data for $T_c = 20.7$ mK show a cusp at T_c, where $C(T)$ crosses over abruptly from quadratic to linear dependence on temperature. This cusp may be the remnant of the fluctuation peak seen for thicker films, in which case it should round out as the superfluid coverage is further reduced. Another possibility is that the heat capacity is singu-

lar even in the absence of order parameter fluctuations. Although this type of behavior would emerge in any mean-field treatment, for an interacting ^{4}He film we would expect a jump discontinuity in $C(T)$ in addition to a change in slope. (The ideal Bose gas should show only a simple cusp at T_c, but of a different form than that seen in Fig. 21.)

VI. CONCLUSIONS

The superfluid density and heat capacity measurements presented in this paper indicate that a ^{4}He film adsorbed on a disordered substrate undergoes a transition from a Bose insulator to a superfluid at the critical coverage n_c. The gap in the insulating phase decreases to zero as the onset coverage is approached from below. Our data show no evidence of a Bose glass phase. In considering thin superfluid films, the rapid change of the chemical potential with coverage near n_c appears to minimize the role of quantum fluctuations, so that the ordinary superfluid transition at T_c remains the dominant critical point. Evidence of critical fluctuations near T_c is seen even for the thinnest superfluid films studied in these experiments.

Although some of the questions raised in this work could be addressed in experiments at even lower temperatures and smaller reduced coverages, the use of different substrates may be more rewarding. We have argued here that the strong substrate potential in porous glasses reduces the importance of quantum fluctuations near the critical coverage. Weakly binding alkali metal substrates[46] may ameliorate this effect. In principle, the use of ordered substrates would allow a test of the clean limit of the various dirty boson models, provided that the adsorption potential is sufficiently weak. Such a system might be achieved by pre-plating a clean high-surface area substrate, such as exfoliated basal-plane graphite, with molecular hydrogen. Finally, even on a strong-binding ordered substrate such as graphite, the adsorption potential changes only weakly within each monolayer, so that quantum effects should be more readily observable. The phase-separated superfluids which exist within the second and third monolayers of ^{4}He on graphite may therefore be reasonable analogs of granular superconductors.[47]

ACKNOWLEDGMENTS

We thank Mary Lanzerotti for assistance with the superfluid density measurements. P.A.C. acknowledges financial support from AT&T Bell Laboratories. This work was supported by the National Science Foundation under Grant Nos. DMR-89-21733 and DMR-93-03855 and by the MRL program of the National Science Foundation under Award No. DMR-91-21654.

*Present address: Department of Physics, University of California, Santa Barbara, CA 93106.

†Present address: NASA Lewis Research Center, 21000 Brookpark Road, Cleveland, OH 44135.

[1] J.E. Berthold, D.J. Bishop, and J.D. Reppy, Phys. Rev. Lett **39**, 348 (1977); D.J. Bishop, J.E. Berthold, J.M. Parpia, and J.D. Reppy, Phys. Rev. B **24**, 5047 (1981).

[2] V. Kotsubo and G.A. Williams, Phys. Rev. B **28**, 440 (1983); Phys. Rev. Lett. **53**, 691 (1984); Phys. Rev. B **33**, 6106 (1986).

[3] H. Cho and G.A. Williams, Phys. Rev. Lett **75**, 1562 (1995).

[4] P.A. Crowell, J. D. Reppy, S. Mukherjee, J. Ma, M.H.W. Chan, and D.W. Schaefer, Phys. Rev. B **51**, 12 721 (1995).

[5] P. Taborek and J.E. Rutledge, Physica B **197**, 2184 (1994), and references therein.

[6] P. A. Crowell and J. D. Reppy, Phys. Rev. B **53**, 2701 (1996).

[7] M.-T. Chen, J.M. Roesler, and J.M. Mochel, J. Low Temp. Phys. **89**, 125 (1992); J.M. Mochel and M.-T. Chen, Phyica B **197**, 278 (1994).

[8] J.D. Reppy, J. Low Temp. Phys. **87**, 205 (1992).

[9] J.L. Hertz, L. Fleishman, and P.W. Anderson, Phys. Rev. Lett. **43**, 942 (1979).

[10] M.P.A. Fisher, P.B. Weichman, G. Grinstein, and D.S. Fisher, Phys. Rev. B **40**, 546 (1989).

[11] M. Ma, B.I. Halperin, and P. Lee, Phys. Rev. B **34**, 3136 (1986); T. Giamarchi and H.J. Schulz, *ibid.* **37**, 325 (1988); D.K.K. Lee and J.M.F. Gunn, J. Phys. Condens. Matter **2**, 7753 (1990); A. Gold, Z. Phys. B **83**, 429 (1991); T. R. Kirkpatrick and D. Belitz, Phys. Rev. Lett **68**, 3232 (1992); K.G. Singh and D.S. Rokhsar, Phys. Rev. B **46**, 3002 (1992); A.P. Kampf and G.T. Zimanyi, *ibid.* **47**, 279 (1993).

[12] G.G. Batrouni, R.T. Scalettar, and G.T. Zimanyi, Phys. Rev. Lett. **65**, 1765 (1990); W. Krauth, N. Trivedi, and D. Ceperley, Phys. Rev. Lett, **67**, 2307 (1991).

[13] B.C. Crooker, B. Hebral, E.N. Smith, Y. Takano, and J.D. Reppy, Phys. Rev. Lett. **51**, 666 (1983).

[14] M.E. Fisher, M.N. Barber, and D. Jasnow, Phys. Rev. A **8**, 1111 (1973).

[15] J.T. Chayes, L. Chayes, D.S. Fisher, and T. Spencer, Phys. Rev. Lett. **57**, 2999 (1986).

[16] P.A. Crowell, M.Y. Lanzerotti, and J.D. Reppy, J. Low Temp. Phys. **89**, 629 (1992).

[17] F.W. Van Keuls, P.A. Crowell, and J.D. Reppy, Physica B **194-196**, 623 (1994).

[18] P.A. Crowell, F.W. Van Keuls, and J.D. Reppy, Phys. Rev. Lett. **75**, 1106 (1995).

[19] Vycor as discussed in this paper is Corning Glass 7930, a precursor to the product sold commercially as Vycor. For a review of the structural properties of Vycor, see P. Levitz, G Ehret, S.K. Sinha, and J.M. Drake, J. Chem. Phys. **95**, 6151 (1991).

[20] *Proceedings of the Fourth International Symposium on Aerogel*, edited by R.W. Pekala and L.W. Hrubesh [J. Noncrystalline Solids **186** (1995)].

[21] G.K.S. Wong, P.A. Crowell, H.A. Cho, and J.D. Reppy, Phys. Rev. B **48**, 3858 (1993).

[22] The films in the aerogel measurements were generally unannealed. Once the critical coverage was exceeded, subsequent doses of ^{4}He were introduced into the cell at low temperature. H. Cho and G.A. Williams (private communication) have noted that annealing of films adsorbed on porous ceramic substrates removed a residual signal above T_c that appeared in unannealed films. All of the coverages in the heat capacity measurements discussed here were annealed.

[23] R.B. Robinson, R. Jochemsen, and J.D. Reppy, Physica B **194-196**, 569 (1994).

[24] D. S. Greywall and P. Busch, Rev. Sci. Instrum. **60**, 471 (1989).

[25] Quantum Design, 11578 Sorrento Valley Road, San Diego, CA 92121-1311.

[26] J.A. Lipa, D.R. Swanson, J.A. Nissen, T.C.P. Chui, and U.E. Israelsson, Phys. Rev. Lett. **76**, 944 (1996), and references therein.
[27] N. Mulders, E. Molz, and J.R. Beamish, Phys. Rev. B **48**, 6293 (1993).
[28] D. Finotello, K.A. Gillis, A. Wong, and M.H.W. Chan, Phys. Rev. Lett. **61**, 1954 (1988); M.H.W. Chan *et al.*, in *Excitations in Two-Dimensional and Three-Dimensional Quantum Fluids*, edited by A.F.G. Wyatt and H.J. Lauter (Plenum, New York, 1991).
[29] S.Q. Murphy and J.D. Reppy, Physica (Amsterdam) B **165&166**, 547 (1990).
[30] B.C. Crooker, Ph.D. thesis, Cornell University, 1984.
[31] D.R. Nelson and J.M. Kosterlitz, Phys. Rev. Lett. **39**, 1201 (1977).
[32] J. Machta and R.A. Guyer, Phys. Rev. Lett. **60**, 2054 (1988); T. Minoguchi and Y. Nagaoka, Prog. Theor. Phys. **80**, 397 (1988).
[33] P. A. Crowell (unpublished).
[34] E.S. Sabisky and C.H. Anderson, Phys. Rev. Lett **30**, 1122 (1973).
[35] D.M. Ceperley, Rev. Mod. Phys. **67**, 279 (1995), discusses the exchange energy for bulk superfluid ^{4}He. We are not aware of a comparable calculation for films but expect that the exchange energy cannot exceed the maximum value ($\sim$ 1.5 K) found for bulk superfluid.
[36] G.T. Zimanyi, P.A. Crowell, R.T. Scalettar, and G.G. Batrouni, Phys. Rev. B **50**, 6515 (1994).
[37] R.H. Tait and J.D. Reppy, Phys. Rev. B **20**, 997 (1979).
[38] A.E. White, R.C. Dynes, and J.P. Garno, Phys. Rev. B **33**, 3549 (1986).
[39] M.A. Paalanen, A.F. Hebard, and R.R. Ruel, Phys. Rev. Lett. **69**, 1604 (1992).
[40] J.M. Valles, Jr., R.C. Dynes, and J.P. Garno, Phys. Rev. Lett **69**, 3567 (1992).
[41] P.A. Crowell, Ph.D. thesis, Cornell University, 1994.
[42] P.B. Weichman, M. Rasolt, M.E. Fisher, and M.J. Stephen, Phys. Rev. B **33**, 4632 (1986); P.B. Weichman, *ibid.* **38**, 8739 (1988); P.B. Weichman and K. Kim, *ibid.* **49**, 813 (1989); a somewhat different approach is adopted by A. Garg, R. Paudit, S. A. Solla, and C. Ebner, *ibid.* **30**, 106 (1984).
[43] J.S. Yoon and M.H.W. Chan (unpublished).
[44] D. Stauffer, M. Ferer, and M. Wortis, Phys. Rev. Lett. **29**, 345 (1972); P.C. Hohenberg, A. Aharony, B.I. Halperin, and E.D. Siggia, Phys. Rev. B **13**, 2986 (1976).
[45] B.D. Josephson, Phys. Lett. **21**, 608 (1966).
[46] M.W. Cole, J. Low Temp. Phys. **101**, 25 (1995); R.B. Hallock, *ibid.* **101**, 31 (1995).
[47] B.A. Huberman and J.G. Dash, Phys. Rev. B **17**, 398 (1978).